Human Molecular Genetics, 2016, Vol. 25, No. 20 4484–4493

doi: 10.1093/hmg/ddw277
Advance Access Publication Date: 18 August 2016
Original Article

ORIGINAL ARTICLE

Mutations in *SDR9C7* gene encoding an enzyme for vitamin A metabolism underlie autosomal recessive congenital ichthyosis

Yohya Shigehara[1], Shujiro Okuda[2], Georges Nemer[3], Adele Chedraoui[4], Ryota Hayashi[1], Fadi Bitar[5], Hiroyuki Nakai[6], Ossama Abbas[7], Laetitia Daou[8], Riichiro Abe[1], Maria Bou Sleiman[7], Abdul Ghani Kibbi[7], Mazen Kurban[3,7,9,†] and Yutaka Shimomura[1,†,*]

[1]Divisions of Dermatology, [2]Division of Bioinformatics, Niigata University Graduate School of Medical and Dental Sciences, Niigata, Japan, [3]Biochemistry & molecular genetics, American University of Beirut Medical Center, Beirut, Lebanon, [4]Department of Dermatology, Lebanese American University-Hospital Rizk, Beirut, Lebanon, [5]Department of Pediatrics, American University of Beirut Medical Center, Beirut, Lebanon, [6]Faculty of Agriculture, Niigata University, Niigata, Japan, [7]Department of Dermatology, [8]Department of Laboratory medicine, American University of Beirut Medical Center, Beirut, Lebanon and [9]Department of Dermatology, Columbia University, New York, NY, USA

*To whom correspondence should be addressed at: Yutaka Shimomura, Division of Dermatology, Niigata University Graduate School of Medical and Dental Sciences, 1-757 Asahimachi-dori, Chuo-ku, Niigata 951-8510, Japan. Tel: +81-25-227-2282; Fax: +81-25-227-0783; Email: yshimo@med.niigata-u.ac.jp

Abstract

Autosomal recessive congenital ichthyosis (ARCI) is a heterogeneous group of hereditary skin disorder characterized by an aberrant cornification of the epidermis. ARCI is classified into a total of 11 subtypes (ARCI1-ARCI11) based on their causative genes or loci. Of these, the causative gene for only ARCI7 has not been identified, while it was previously mapped on chromosome 12p11.2-q13.1. In this study, we performed genetic analyses for three Lebanese families with ARCI, and successfully determined the linkage interval to 9.47 Mb region on chromosome 12q13.13-q14.1, which was unexpectedly outside of the ARCI7 locus. Whole-exome sequencing and the subsequent Sanger sequencing led to the identification of missense mutations in short chain dehydrogenase/reductase family 9C, member 7 (*SDR9C7*) gene on chromosome 12q13.3, i.e. two families shared an identical homozygous mutation c.599T > C (p.Ile200Thr) and one family had another homozygous mutation c.214C > T (p.Arg72Trp). In cultured cells, expression of both the mutant SDR9C7 proteins was markedly reduced as compared to wild-type protein, suggesting that the mutations severely affected a stability of the protein. In normal human skin, the SDR9C7 was abundantly expressed in granular and cornified layers of the epidermis. By contrast, in a patient's skin, its expression in the cornified layer was significantly decreased. It has previously been reported that SDR9C7 is an enzyme to convert retinal into retinol. Therefore, our study not only adds a new gene responsible for ARCI, but also further suggests a potential role of vitamin A metabolism in terminal differentiation of the epidermis in humans.

[†]These authors equally contributed to this work.

Received: May 25, 2016. **Revised:** July 16, 2016. **Accepted:** August 15, 2016

Introduction

Autosomal recessive congenital ichthyosis (ARCI) is a genetically heterogeneous disorder of epidermal keratinization of the skin. ARCI is clinically characterized by dryness and scaling of the whole body surface. Pathologically, the conditions are considered to be due to dysfunction of underlying keratinocyte differentiation, which results in the characteristic distinctive scaling skin (1). The clinical conditions vary according to each type of the ichthyosis, while it is often too hard to determine the causative gene based on clinical features. To date, a total of 10 genes responsible for ARCI have been identified, which are *TGM1* (ARCI1; MIM 242300) (2,3), *ALOX12B* (ARCI2; MIM 242100) (4), *ALOXE3* (ARCI3; MIM 606545) (4), *ABCA12* (ARCI4; MIM 601277/242500) (5,6), *CYP4F22* (ARCI5; MIM 604777) (7), *NIPAL4* (ARCI6; MIM 612281) (8), *LIPN* (ARCI8; MIM 613943) (9), *CERS3* (ARCI9; MIM 615023) (10), *PNPLA1* (ARCI10; MIM 615024) (11), and *ST14* (ARCI11; MIM 602400) (12). In addition, ARCI has also previously been mapped on chromosome 12p11.2-q13 (ARCI7; MIM 615022); the causative gene, however, has not yet been reported (13).

In the present study, we performed extensive genetic analyses for three consanguineous Lebanese families with ARCI (Families 1–3). We mapped the susceptible locus of these families to chromosome 12q13.13-q14.1, which was just outside of the ARCI7 locus. Through whole-exome sequencing and Sanger sequencing, we identified missense mutations in short chain dehydrogenase/reductase family 9C, member 7 (*SDR9C7*) gene on chromosome 12q13.3 in all the three families analyzed. Furthermore, we investigated how the mutations affected expression of SDR9C7 protein both *in vitro* and *in vivo*.

Results

Clinical description

Patients in all the three families have had large erythematous scales on the whole body surface, particularly over the trunk with hyperkeratosis affecting elbows and knees since birth (Fig. 1A–E). During the first few years of life, the condition was the worst. The individuals that we encountered during the second, third, fourth and fifth decades of their lives had similar skin features, but to a much lesser extent than those in their first decade of life and the severity decreased accordingly with age. Around 25–30% of the patients we encountered in their first decade of life also had mild-moderate facial and scalp involvement (Fig. 1F), while the others had sparing of the face and scalp. Palmoplantar hyperkeratosis and extensor hyperkeratosis were evident in most of the patients (Fig. 1G), while they did not show flexion contractures. In addition, persistent fungal skin infections that started early during the first decade of life were present in most affected individuals. The infections responded to itraconazole and terbinafine, but consistently recurred a few weeks after stopping the antifungal medications. About 50% of the patients also had onychomycosis (Fig. 1H). We performed KOH smears for all these cases with fungal infections. Furthermore, nail and skin cultures were made from two patients that confirmed infection with dermatophytic trichophyton species. The fungal infections were less frequent after the first decade of life, yet continued to happen. None of the affected individuals showed any other associated findings, such as hypotrichosis, ocular involvement, or mental retardation. Biopsy specimen from an affected individual of Family 2 showed a mild hypergranulosis and a marked hyperkeratosis of the epidermis, which were compatible for lamellar ichthyosis (Fig. 1I).

Results of initial haplotype analysis and whole-exome sequencing

Using the genomic DNA of the family members as templates, we performed haplotype analysis with microsatellite markers around all the 10 known genes for ARCI. None of the families, however, showed linkage to any of these genes (data not shown). We then forwarded to analyze the ARCI7 locus on chromosome 12 for these families. We initially found that affected individuals in Family 1 finely showed a homozygous haplotype within and around the ARCI7 locus (Supplementary Material, Fig. S1). On the other hand, Families 2 and 3 were excluded from the ARCI7 locus (data not shown). Based on recombination events, the linkage interval of Family 1 was defined to be 45.0 Mb in size, flanked by markers D12S1648 and D12S1660, which almost completely included the ARCI7 locus (Supplementary Material, Fig. S1). Subsequently, we performed whole-exome sequencing using genomic DNA from 1 affected and 1 unaffected (carrier) members of Family 1, and analyzed the data. Within the linkage interval between markers D12S1648 and D12S1660, we identified 363 and 482 single nucleotide variants (SNVs) in the affected and the carrier individuals, respectively. Of these SNVs, we searched for genes with non-synonymous rare variants (minor allele frequency ≤ 0.01) that were homozygous and heterozygous in the affected and the carrier individuals, respectively. As a result, a total of 5 genes, *WNT1*, *SDR9C7*, *MON2*, *HELB* and *GLIPR1L2*, were extracted (Table 1). To our surprise, however, all these candidate genes did not residue within the ARCI7 locus. Instead, they were located downstream of the ARCI7 locus (Table 1).

Results of additional haplotype analysis

At that point, we re-checked the results of haplotype analysis of Families 2 and 3 and noticed that a part of the region downstream of the ARCI7 locus looked showing a homozygous haplotype in both families (data not shown). Therefore, we put more microsatellite markers on chromosome 12q13-q14 and performed the haplotype analysis again. Strikingly, the results demonstrated that all the three families clearly linked to this locus (Fig. 2). In particular, critical recombination events were detected between markers D12S96 and D12S398, as well as between markers D12S1056 and MON2-MS1 in Family 2, which allowed the linkage interval to be limited to 9.47 Mb in size, flanked by markers D12S96 and MON2-MS1 (Figs. 2B and 3A).

Identification of rare variants in the *SDR9C7* gene in all the three families

When we looked back to the results of exome sequencing of Family 1, we found that a rare variant in the *SDR9C7* gene was only included in the renewed linkage interval (Fig. 3A, Table 1). This variant was a nucleotide substitution in exon 3 of the *SDR9C7* gene (c.599T $\geq$ C; p.Ile200Thr; rs770729222). We performed Sanger sequencing and confirmed that members of Family 1 definitely carried this variant (Fig. 3B). Subsequently, using the genomic DNA from members of Families 2 and 3, we amplified all exons and exon-intron boundary sequences of the *SDR9C7* by polymerase chain reaction (PCR), and directly-sequenced the PCR products. The results demonstrated that

Figure 1. Clinical and histological features of patients with ARCI. (**A–H**) Affected individuals in all the three families have had dry skin with large scales on the whole body surface, hyperkeratosis over elbows and knees, palmoplantar keratoderma and recurrent dermatophytic infections of the skin and onychomycosis. (A,B,F) 10-year-old girl in Family 1. (C,D) 9-year-old girl in Family 2. (E) 19-year-old male in Family 3. (G)(H) 13-year-old girl in Family 1. (**I**) Histological features of a skin biopsy from the affected individual of Family 2 was compatible for lamellar ichthyosis. Hematoxylin-eosin staining. Scale bar: 100 μm.

Family 2 had a missense variant c.214C > T (p.Arg72Trp; rs530109812) in exon 1 (Fig. 3C), and Family 3 carried c.599T > C (p.Ile200Thr) in exon 3 of the *SDR9C7* gene, respectively (data not shown). It is noteworthy that Family 3 had the identical *SDR9C7* variant with Family 1, which reflected the fact that Families 1 and 3 were from the same region in Lebanon and they shared an identical haplotype around the *SDR9C7* gene (Fig. 2A and C). Screening assays with restriction enzymes revealed that both the variants completely co-segregated with the disease phenotype and were excluded from 300 population-matched unrelated unaffected individuals (600 chromosomes) (Supplementary Material, Fig. S2; data not shown).

Table 1. The results of whole-exome sequencing for Family 1: List of non-synonymous rare variants that were homozygous and heterozygous in affected and unaffected (carrier) individuals, respectively

Ch12 position (NC_000012.12)	48,979,627 bp	56,929,515 bp	62,532,629 bp	66,310,496 bp	75,422,951 bp
Reference allele	T	A	A	A	G
Alternate allele	A	G	G	C	A
dbSNP rs#	rs61758378	rs770729222	rs143346269	rs141956990	rs144813686
Gene	*WNT1*	*SDR9C7*	*MON2*	*HELB*	*GLIPR1L2*
cDNA change	c.264T>A	c.599T>C	c.1592A>G	c.1568A>C	c.632G>A
Amino acid change	p.Ser88Arg	p.Ile200Thr	p.Gln531Arg	p.Gln523Pro	p.Arg211Gln
Variant type	missense	missense	missense	missense	Missense
ExAC-MAF	0.0030	0.000008	0.0005	0.0178	0.0004
1000 Genomes-MAF	0.0028	N/A	0.0010	0.0088	0.0006
SIFT score (result)	0.46 (tolerated)	0.02 (deleterious)	0.26 (tolerated)	0.09 (tolerated)	0.9 (tolerated)
PolyPhen-2 score (result)	0.124 (benign)	0.701 (possibly damaging)	0 (benign)	0.864 (possibly damaging)	0.004 (benign)

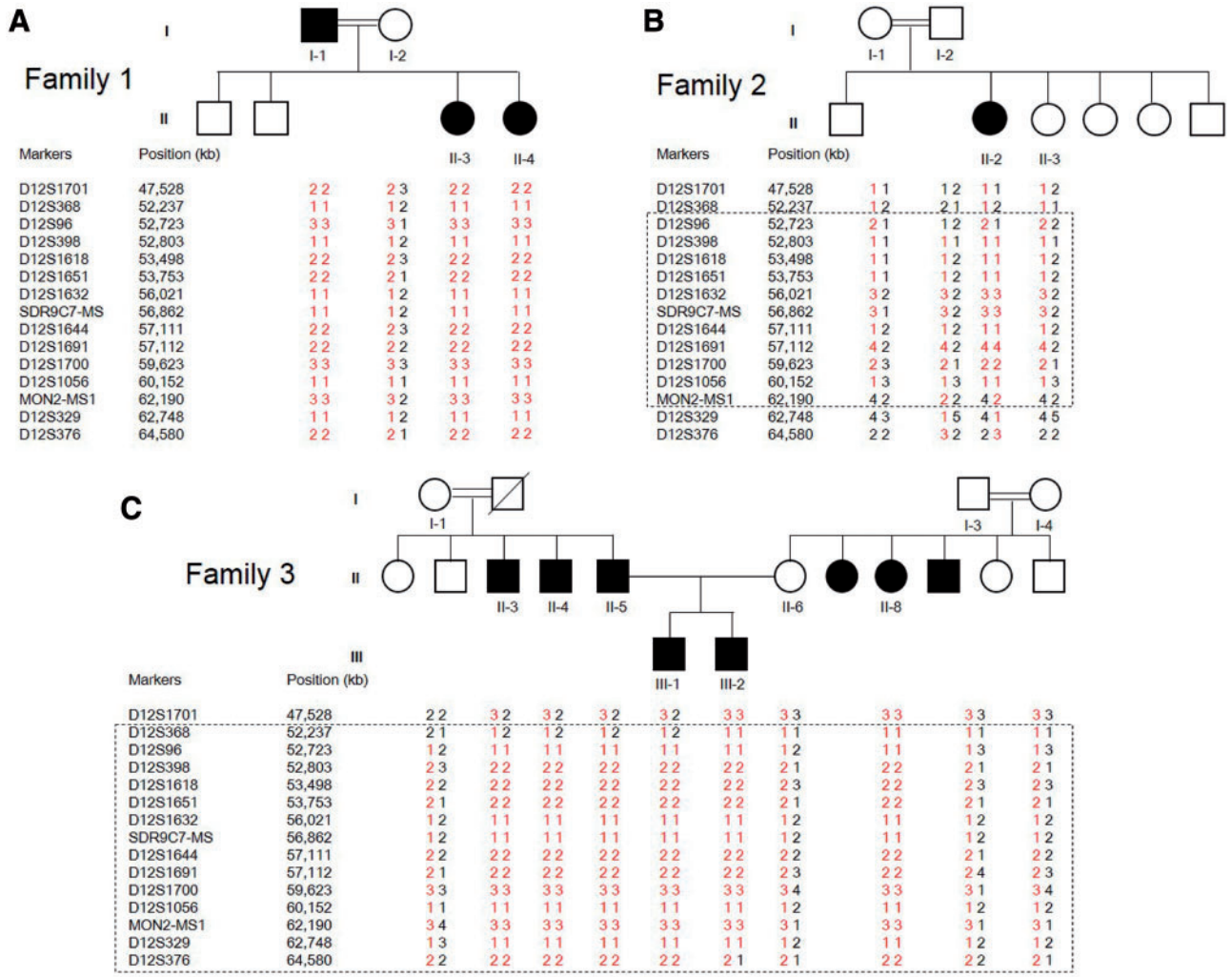

Figure 2. Fine mapping of ARCI phenotype on chromosome 12q13.13-q14.1. Pedigrees and Results of haplotype analysis for Family 1 (**A**), Family 2 (**B**), and Family 3 (**C**). Disease-related haplotypes are coloured in red. The linkage interval defined in Families 2 and 3 is indicated by dotted squares (B, C).

Expression of the mutant SDR9C7 proteins in cultured cells

Human SDR9C7 protein consists of a total of 313 amino-acid residues, and multiple amino acid sequence alignment of SDR9C7 revealed that both 72Arg and 200Ile were highly conserved among different species (Supplementary Material, Fig. S3). Furthermore, both Arg to Trp substitution at codon 72 and Ile to Thr substitution at codon 200 were predicted to be

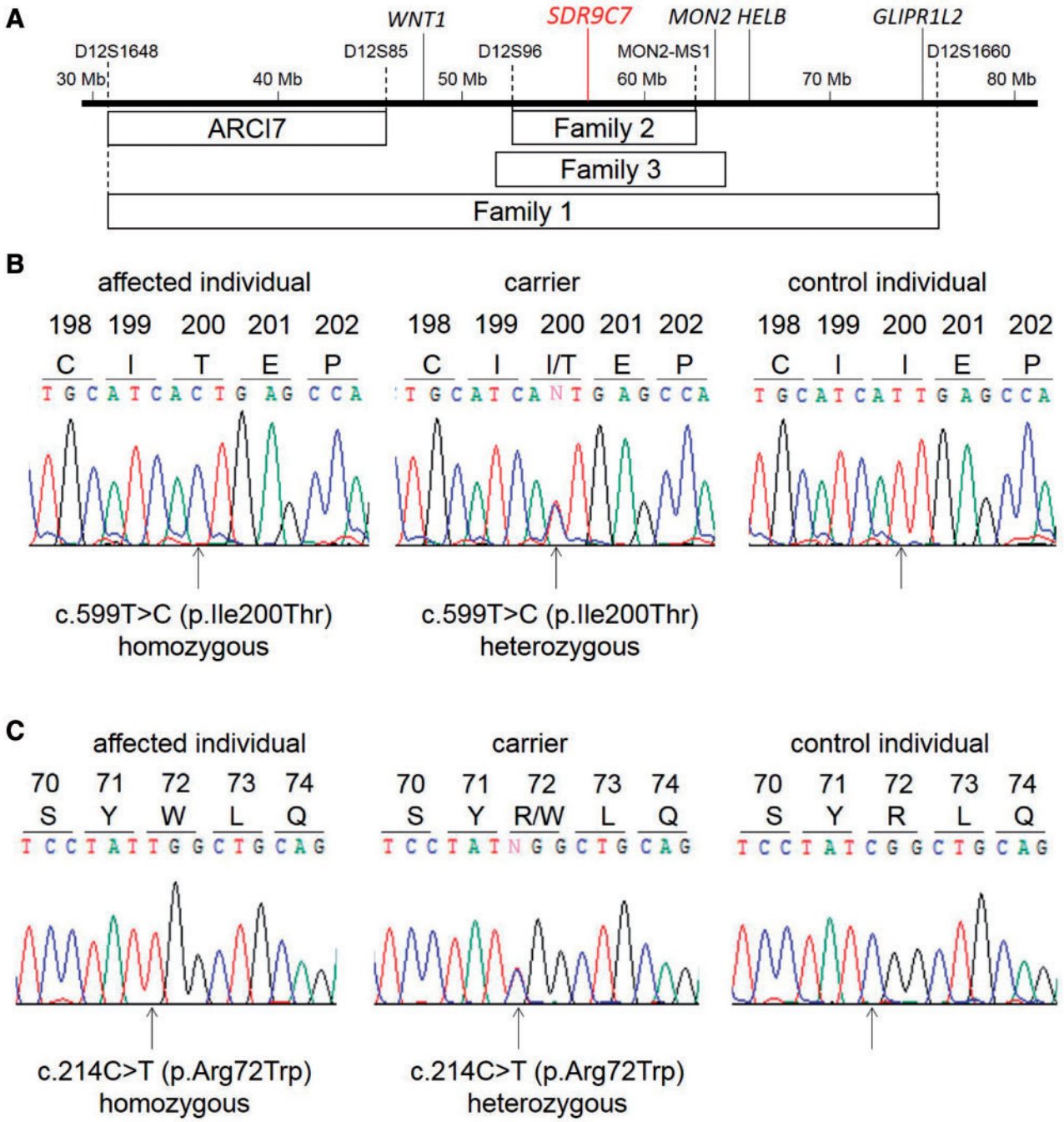

Figure 3. Identification of rare variants in the *SDR9C7* gene. (**A**) Schematic representation of the position of the ARCI7 locus and the linkage interval of Families 1–3 determined in this study. Position of the candidate genes and microsatellite markers is shown on the top. The *SDR9C7* gene is coloured in red. Note that the linkage interval of Families 2 and 3 are apart from the ARCI7 locus. (**B**) Identification of a homozygous rare variant c.599T>C (p.Ile200Thr) in the *SDR9C7* gene of Family 1. (**C**) Identification of a homozygous rare variant c.214C>T (p.Arg72Trp) in the *SDR9C7* gene of Family 2.

deleterious by SIFT and possibly damaging by PolyPhen-2, respectively (Table 1, Supplementary Material, Table S1). In order to analyze how the missense variants p.Arg72Trp and p.Ile200Thr affected their expression, we overexpressed wild-type (Wt) or the two mutant (Mut) SDR9C7 proteins in HEK293T cells, and analyzed their expression by western blots (WBs) with two distinct mouse monoclonal anti-SDR9C7 antibodies (clones 10B4 and 4B5; LifeSpan BioSciences, Inc., Seattle, WA, USA). We initially confirmed that the epitope of each antibody was located within amino acid residues 106-210 of the SDR9C7 protein (Supplementary Material, Fig. S4). In addition, we also overexpressed N-terminal Flag-tagged SDR9C7 proteins in the cells and peformed WBs with an anti-Flag antibody. The results demonstrated that expression levels of both the Mut proteins were significantly reduced as compared to the Wt protein (Fig. 4), suggesting an instability of the Mut proteins. The sum of these results suggests that both p.Arg72Trp and p.Ile200Thr are not non-consequential rare

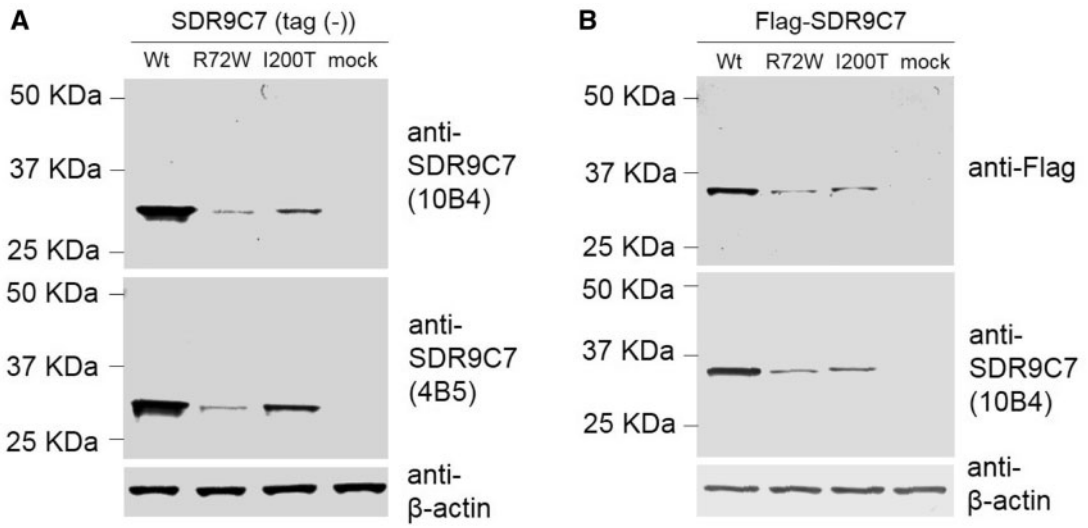

Figure 4. Expression studies of SDR9C7 in cultured cells. (**A**) Wild-type (Wt), as well as R72W and I200T mutant SDR9C7, without any tags (Tag (-)) were overexpressed in HEK293T cells, and were detected by western blots (WBs) with two distinct anti-SDR9C7 antibodies (clones 10B4 and 4B5). (**B**) N-terminal Flag-tagged SDR9C7 proteins were overexpressed in HEK293T cells and were analyzed by WBs with anti-Flag and anti-SDR9C7 (clone 10B4) antibodies. WB with anti-β-actin antibody was also performed to show equal loading (A,B). The results clearly demonstrated that expression level of both the mutant proteins was much lower than that of Wt protein.

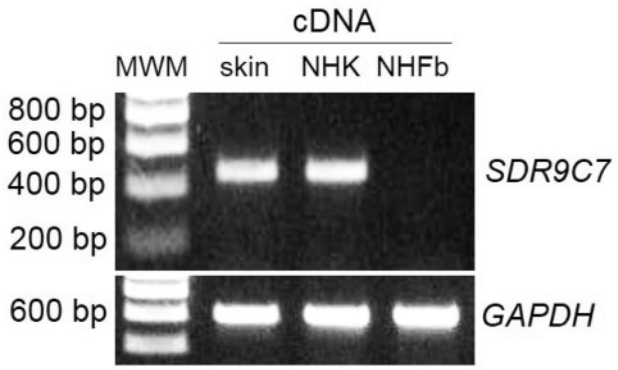

Figure 5. Results of RT-PCR. Expression of the *SDR9C7*-mRNA was detected in the skin and normal human keratinocyte (NHK), but not in normal human fibroblast (NHFb). *GAPDH* was amplified as a positive control.

variants, but pathogenic mutations responsible for ARCI in Families 1-3.

Expression of the *SDR9C7*-mRNA in human skin

To investigate the expression of the *SDR9C7*-mRNA in human skin, we performed reverse-transcription (RT)-PCR using total RNA from a skin sample of a healthy control individual, normal human keratinocyte (NHK) and fibroblast (NHFb). The *SDR9C7*-cDNA was amplified from the skin and NHK, but not from NHFb (Fig. 5). The results showed that the *SDR9C7*-mRNA was expressed in human skin, and also suggested that it would mainly be expressed in the epithelial components.

Localization of the SDR9C7 protein in human skin

Finally, in order to precisely localize the SDR9C7 expression in human skin, we performed indirect-immunofluorescence (IIF) studies on skin sections from a healthy control individual and an affected individual from Family 2 with a homozygous mutation c.214C > T (p.Arg72Trp) in the *SDR9C7* gene. In normal skin, SDR9C7 was predominantly expressed in granular and conrnified layers of the epidermis (Fig. 6A and B, Supplementary Material, Fig. S5). In the patient's skin, SDR9C7 expression was detected in the granular layer, similar to the normal skin. However, it was only weakly detected in the cornified layer, which implied an aberrant expression of the Mut-SDR9C7 protein during terminal differentiation of the epidermis (Fig. 6C and D). We also analyzed expression patterns of several differentiation markers of the epidermis. We did not see obvious differences in expression of loricrin or keratin 1 between affected and unaffected individuals (Fig. 6A–D, Supplementary Material, Fig. S6). By contrast, expression of involucrin and filaggrin looked more abundant in the affected individual (Supplementary Material, Fig. S6), which might be due to hypergranulosis in the patient's epidermis.

Discussion

In this study, we found three Lebanese families with ARCI without showing linkage to any known causative genes, and identified mutations in the *SDR9C7* gene in all the three families analyzed. The SDR9C7 protein, previously known as SDR-O, belongs to the SDR enzyme superfamily (14,15). Although amino acid sequences of SDR9C7 do not show high homology with any other SDR proteins, it has characteristic structural and sequence motifs common for SDR proteins, i.e. the α/β folding motif Rossmann-fold, the glycine rich cofactor binding motif TGxxxGxG and the active centre motif YxxxK (14). It is less likely that the mutations p.Arg72Trp and p.Ile200Thr identified in this study directly affect the latter two sequence motifs. However, based on the crystal structure of an SDR member 17-β-hydroxysteroid dehydrogenase type 1 (17-β-HSD1) (PDB ID 1i5rA), 200Ile in SDR9C7 protein corresponding to 183Ile in α6 of 17-β-HSD1 is predicted to be critical for stabilization of the structural motif via a hydrophobic interaction with the 264Met corresponding to 240Phe in β6 of 17-β-HSD1 (16,17). The substitution

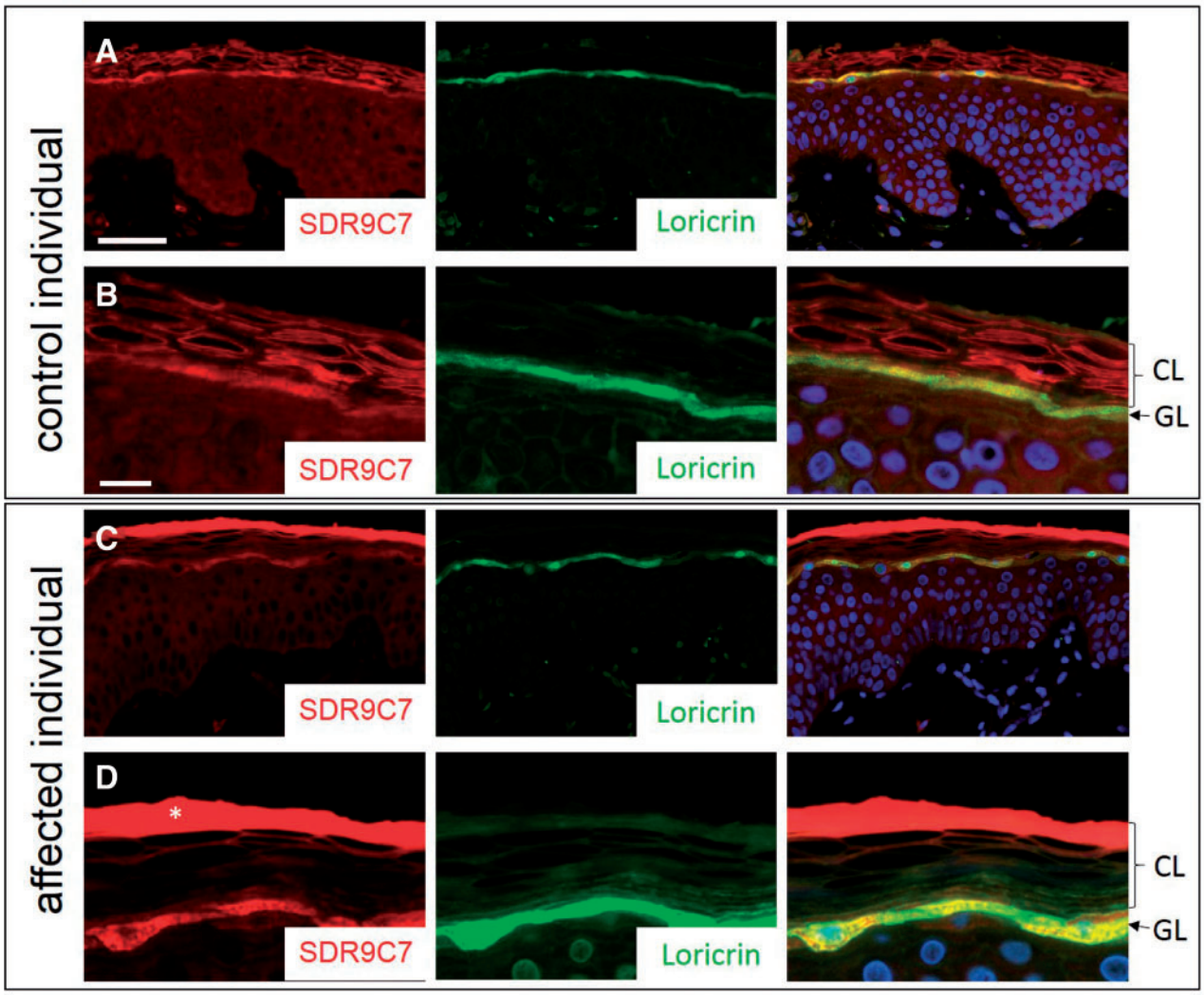

Figure 6. Results of indirect-immunofluorescence (IIF) on skin sections. (**A–D**) We performed double-IIF studies with mouse monoclonal anti-SDR9C7 clone 10B4 (left panels) and rabbit polyclonal anti-loricrin (middle panels) antibodies on paraffin sections of a healthy control individual (A, B) and an affected individual of Family 2 (C, D). The right panels are merged images, and counterstaining with DAPI is shown in blue. SDR9C7 was expressed in granular layer (GL) and cornified layer (CL) of the epidermis in the control skin (A, B). In contrast, SDR9C7 expression in the cornified layer was much lower in the patient's skin (C, D). Note that a strong red signal in the uppermost cornified layer in the patient's epidermis (asterisk in panel D) turned out to be a background as it was also detected in stainings without applying primary antibodies (data not shown). There were no obvious differences in expression of loricrin between the control and the affected individuals (middle panels). Scale bars: 100 μm (A), 20 μm (B).

from Ile (non-polar) to Thr (polar) at the amino acid residue 200 most likely disrupts the hydrophobic interaction, severely affecting the conformation of the SDR9C7 protein including the Rossmann-fold, which is supported by reduced expression of the p.Ile200Thr-Mut SDR9C7 *in vitro* (Fig. 4). Concerning the mutation p.Arg72Trp, it was hard to precisely predict the effect on the conformation, because of difficulty in performing a reliable homology modelling. Nevertheless, marked reduction of the p.Arg72Trp-Mut protein both *in vitro* and *in vivo* suggested that the mutation would result in disruption of the protein structure (Figs. 4, 6C and D).

SDR proteins are known to catalyze activation/inactivation of prostaglandins, retinoids and several classes of steroid hormones, and as such they catalyze metabolism of various ligands for nuclear receptors (18). Although little is known about the cofactor and the substrate of SDR9C7 protein, it has been reported that SDR9C7 showed a weak activity to convert retinal into retinol in the presence of the cofactor NADH (18). Therefore, SDR9C7 appears to be involved in vitamin A metabolism, while it may also have additional functions. In this study, we have shown that SDR9C7 is abundantly expressed in the granular and the cornified layers of the epidermis where the epidermal keratinocytes are terminally differentiated (Fig. 6A and B, Supplementary Material, Fig. S5). An importance of the vitamin A metabolism in the epidermal differentiation can easily be expected because of the fact that derivatives of vitamin A are widely used for treatment of various cutaneous disorders including ichthyosis. In addition, it is noteworthy that patients with *SDR9C7* mutations tend to have recurrent fungal skin infections, suggesting that SDR9C7 is largely involved in barrier function of the epidermis, especially to prevent fungal infections. However, it remains unknown why the patients did not frequently suffer from bacterial, viral or candidal infections. It might be because the deformity of the skin barrier did not affect

the innate immunity against these infections including cathelicidins and defensins for instance.

Our data not only provide a novel causative gene for ARCI, but also raise a possibility that SDR9C7 can become a new therapeutic molecule for various cutaneous disorders, even though further analyzes are definitely required to reveal the precise role of SDR9C7 in the epidermis, as well as the functional consequences resulting from the *SDR9C7* mutations identified in this study.

Materials and Methods

DNA extraction

Informed consent was obtained from all subjects and approval for this study was provided by the Institutional Review Board of Niigata University and American University of Beirut Medical Center. The study was conducted in adherence to the Declaration of Helsinki Principles. Peripheral blood samples were collected from the family members as well as unrelated healthy control individuals of Lebanese origin, and genomic DNA was extracted from each sample with the QIAamp DNA Blood Midi Kit (Qiagen Inc., Valencia, CA, USA).

Haplotype analysis

Using the genomic DNA from the family members as templates, microsatellite markers close to all the known genes for ARCI (ARCI1-6 and ARCI8-11), as well as those for the ARCI7 locus on chromosome 12, were amplified by PCR. The PCR products were analyzed on 8% polyacrylamide gels, and genotypes were determined by visual inspection.

Whole-exome sequencing

Whole-exome sequencing was performed using genomic DNA from members of Family 1 and the SureSelect Human All Exon V5 Kit (Agilent Technologies, Santa Clara, CA, USA) following the manufacture's recommendations. Alignment was performed to the hg19 reference genome with Burrows-Wheeler Aligner (BWA) (19), and it was processed with SAMtools (20) and Picard. Genome Analysis Toolkit (GATK) (21) was applied to base quality score recalibration, indel realignment, duplicate removal, and SNVs and indels discovery. Variants were annotated with SnpEff (22) and ANNOVAR (23).

Mutation analysis of *SDR9C7* gene

Using the genomic DNA from the family members as templates, all exons including exon-intron boundaries of the *SDR9C7* gene were PCR-amplified using gene specific primers (Supplementary Material, Table S2). The amplified PCR products were directly-sequenced in an ABI 3130xl genetic analyzer using the ABI Prism Big Dye Terminator Cycle Sequencing Ready Reaction Kit (PE Applied Biosystems, Foster City, CA, USA).

Screening assays for the *SDR9C7* variants

To screen for the variant c.599T > C (p.Ile200Thr) in the *SDR9C7* gene, intron 2-exon 3 boundary sequences of the *SDR9C7* were amplified by PCR using a forward primer (5'-ACAGGGGT GAGAGAAGCATC-3') and a reverse primer (5'-TGACTCCAG GTTCTCCTTGC-3'). The PCR products were digested by a restriction enzyme *Dde*I at 37 °C for 3 h, and analyzed on 8.0% polyacrylamide gels. For the variant c.214C > T (p.Arg72Trp), exon 1-intron 1 boundary sequences of the *SDR9C7* were PCR-amplified using a mismatch forward primer (5'-GAGGGAT CCCAGAAACTTCAGCGGGATACCTCCGA-3') and a reverse primer (5'-CATGCAGTGGCTTCCAATCAG-3'). Note that a T > G nucleotide substitution was introduced into the forward primer to generate a *Pvu*I restriction enzyme site only in PCR products from Wt alleles (underlined). The PCR products were digested with *Pvu*I at 37 °C for 3 h, and analyzed on 7.5% polyacrylamide gels.

Generation of expression vectors

Using first-strand cDNA generated from total RNA of normal human skin as a template, cDNA sequences containing the full-length coding region of the *SDR9C7* were amplified by PCR using primers listed on Supplementary Material, Table S2. The amplified product was cloned into *Eco*RI and *Xho*I sites of the mammalian expression vectors pCXN2.1 (24) and pCMV-Tag2A (Agilent Technologies, Santa Clara, CA). The expression constructs for the p.Arg72Trp and the Ile200Thr Mut-SDR9C7 were generated using the QuikChange II XL Site-Directed Mutagenesis Kit (Agilent Technologies, Santa Clara, CA, USA) and the Wt-SDR9C7-expression vectors as a template.

SDR9C7-cDNA sequences encoding amino acid residues 1-105, 106-210 and 211-313 were PCR-amplified using the pCXN2.1-Wt-SDR9C7 vector as a template (Supplementary Material, Table S2). The PCR products were subsequently cloned into *Eco*RI and *Sal*I sites of the pEGFP-C1 vector (Takara Bio Inc., Shiga, Japan) which expresses N-terminal GFP-tagged proteins.

Transient transfection and WBs

HEK293T cells were cultured in Dulbecco's modified Eagle's medium (Invitrogen, Carlsbad, CA, USA) supplemented with 10% fetal bovine serum, 100 IU/ml penicillin and 100 μg/ml streptomycin. Cells were plated in 35-mm dishes on the day before transfection. Expression vectors were transfected into the cells using lipofectamine 2000 (Invitrogen). Cells were harvested 24 h after the transfection. The total cell lysate was separated on 4–12% NuPAGE gels (Invitrogen), and WBs were subsequently performed according to a previously described method (25). The primary antibodies used were mouse monoclonal anti-SDR9C7 clone 10B4 (diluted 1:1,000; LifeSpan BioSciences, Inc.), mouse monoclonal anti-SDR9C7 clone 4B5 (diluted 1:500; LifeSpan BioSciences, Inc.), mouse monoclonal anti-Flag (diluted 1:1,000; Sigma-Aldrich, St. Louis, MO, USA), rabbit polyclonal anti-GFP (diluted 1:2,000; MBL, Nagoya, Japan), and rabbit polyclonal anti-β-actin (diluted 1:3,000; Sigma-Aldrich).

RT-PCR

Total RNA was extracted from a skin sample of a healthy control individual, as well as cultured NHK and NHFb, using the RNeasy Mini Kit (Qiagen). Note that NHK was cultured in a medium containing 1.2 mM $CaCl_2$ in order to induce differentiation. The total RNA was subsequently reverse-transcribed with oligo-dT primers and Superscript III (Invitrogen). Using the first-strand cDNA as a template, cDNA sequences of the *SDR9C7* and the *GAPDH* genes were amplified by PCR using gene-specific primers (Supplementary Material, Table S2). The PCR products were run on 1.0% agarose gels.

IIF studies

IIF studies were performed on paraffin or fresh frozen sections following the methods described previously with minor modifications (25,26). The primary antibodies used were mouse monoclonal anti-SDR9C7 clone 10B4 (diluted 1:100; LifeSpan BioSciences, Inc.), mouse monoclonal anti-SDR9C7 clone 4B5 (diluted 1:150; LifeSpan BioSciences, Inc.), rabbit polyclonal anti-loricrin (diluted 1:200; Novus Biologicals, Littleton, CO, USA), rabbit polyclonal anti-involucrin (diluted 1:500; Abcam, Cambridge, MA, USA), mouse monoclonal anti-filaggrin (clone SPM181; prediluted; GeneTex, Irvine, CA, USA), and rabbit polyclonal anti-keratin 1 (diluted 1:500; BioLegend Inc., San Diego, CA, USA).

Web resources

The URLs for data presented herein are as follows.

Online Mendelian Inheritance in Man (OMIM): http://www.ncbi.nlm.nih.gov/Omim/

GenBank: http://www.ncbi.nlm.nih.gov/Genbank/

PubMed: www.ncbi.nlm.nih.gov/sites/entrez

Ensembl Genome Browser: http://www.ensembl.org/

SIFT: http://sift.jcvi.org/

PolyPhen-2: http://genetics.bwh.harvard.edu/pph2/

Picard: http://broadinstitute.github.io/picard/

dbSNP: http://www.ncbi.nlm.nih.gov/projects/SNP/

RCSB Protein Data Bank (PDB): http://www.rcsb.org/pdb/home/home.do

Supplementary Material

Supplementary Material is available at *HMG* online.

Acknowledgements

We acknowledge the family members involved in this study. We thank Drs. Satoshi Ishii (Akita University, Japan) and Junichi Miyazaki (Osaka University, Japan) for supplying pCXN2.1 vector.

Conflict of Interest statement. None declared.

Funding

This study was supported in part by a grant from the Naito Foundation, Japan (to Y.S.) and by an MPP and URB grants from the American University of Beirut Medical Center (to M.K.).

References

1. Takeichi, T. and Akiyama, M. (2016) Inherited ichthyosis: non-syndromic forms. *J. Dermatol.*, **43**, 242–251.
2. Huber, M., Rettler, I., Bernasconi, K., Frenk, E., Lavrijsen, S.P., Ponec, M., Bon, A., Lautenschlager, S., Schorderet, D.F. and Hohl, D. (1995) Mutations of keratinocyte transglutaminase in lamellar ichthyosis. *Science*, **267**, 525–528.
3. Russel, L.J., DiGiovanna, J.J., Rogers, G.R., Steinert, P.M., Hashem, N., Compton, J.G. and Bale, S.J. (1995) Mutations in the gene for transglutaminase 1 in autosomal recessive lamellar ichthyosis. *Nat. Genet.*, **9**, 279–283.
4. Jobard, F., Lefèvre, C., Karaduman, A., Blanchet-Bardon, C., Emre, S., Weissenbach, J., Ozgüc, M., Lathrop, M., Prud'homme, J.F. and Fischer, J. (2002) Lipoxygenase-3 (*ALOXE3*) and 12 (*R*)-lipoxygenase (*ALOX12B*) are mutated in non-bullous congenital ichthyosiform erythroderma (NCIE) linked to chromosome 17p13.1. *Hum. Mol. Genet.*, **11**, 107–113.
5. Lefèvre, C., Audebert, S., Jobard, F., Bouadjar, B., Lakhdar, H., Boughdene-Stambouli, O., Blanchet-Bardon, C., Heilig, R., Foglio, M., Weissenbach, J., *et al.* (2003) Mutations in the transporter *ABCA12* are associated with lamellar ichthyosis type 2. *Hum. Mol. Genet.*, **12**, 2369–2378.
6. Kelsell, D.P., Norgett, E.E., Unsworth, H., Teh, M.T., Cullup, T., Mein, C.A., Dopping-Hepenstal, P.J., Dale, B.A., Tadini, G., Fleckman, P., *et al.* (2005) Mutations in *ABCA12* underlie the severe congenital skin disease harlequin ichthyosis. *Am. J. Hum. Genet.*, **76**, 794–803.
7. Lefèvre, C., Bouadjar, B., Ferrand, V., Tadini, G., Mégarbané, A., Lathrop, M., Prud'homme, J.F. and Fischer, J. (2006) Mutations in a new cytochrome P450 gene in lamellar ichthyosis type 3. *Hum. Mol. Genet.*, **15**, 767–776.
8. Lefèvre, C., Bouadjar, B., Karaduman, A., Jobard, F., Saker, S., Ozguc, M., Lathrop, M., Prud'homme, J.F. and Fischer, J. (2004) Mutations in ichthyin a new gene on chromosome 5q33 in a new form of autosomal recessive congenital ichthyosis. *Hum. Mol. Genet.*, **13**, 2473–2482.
9. Israeli, S., Khamaysi, Z., Fuchs-Telem, D., Nousbeck, J., Bergman, R., Sarig, O. and Sprecher, E. (2011) A mutation in *LIPN*, encoding epidermal lipase N, causes a late-onset form of autosomal-recessive congenital ichthyosis. *Am. J. Hum. Genet.*, **88**, 482–487.
10. Radner, F.P., Marrakchi, S., Kirchmeier, P., Kim, G.J., Ribierre, F., Kamoun, B., Abid, L., Leipoldt, M., Turki, H., Schempp, W., *et al.* (2013) Mutations in *CERS3* cause autosomal recessive congenital ichthyosis in humans. *PLoS Genet.*, **9**, e1003536.
11. Grall, A., Guaguère, E., Planchais, S., Grond, S., Bourrat, E., Hausser, I., Hitte, C., Le Gallo, M., Derbois, C., Kim, G.J., *et al.* (2012) *PNPLA1* mutations cause autosomal recessive congenital ichthyosis in golden retriever dogs and humans. *Nat. Genet.*, **44**, 140–147.
12. Basel-Vanagaite, L., Attia, R., Ishida-Yamamoto, A., Rainshtein, L., Ben Amitai, D., Lurie, R., Pasmanik-Chor, M., Indelman, M., Zvulunov, A., Saban, S., *et al.* (2007) Autosomal recessive ichthyosis with hypotrichosis caused by a mutation in *ST14*, encoding type II transmembrane serine protease matriptase. *Am. J. Hum. Genet.*, **80**, 467–477.
13. Mizrachi-Koren, M., Geiger, D., Indelman, M., Bitterman-Deutsch, O., Bergman, R. and Sprecher, E. (2005) Identification of a novel locus associated with congenital recessive ichthyosis on 12p11.2-q13. *J. Invest. Dermatol.*, **125**, 456–462.
14. Chen, W., Song, M.S. and Napoli, J.L. (2002) SDR-O: an orphan short-chain dehydrogenase/reductase localized at mouse chromosome 10/human chromosome 12. *Gene*, **294**, 141–146.
15. Kavanagh, K.L., Jörnvall, H., Persson, B. and Oppermann, U. (2008) Medium- and short-chain dehydrogenase/reductase gene and protein families: the SDR superfamily: functional and structural diversity within. *A Family of Metabolic and Regulatory Enzymes. Cell Mol. Life Sci.*, **65**, 3895–3906.
16. Mazza, C., Breton, R., Housset, D. and Fontecilla-Camps, J.C. (1998) Unusual charge stabilization of NADP+ in 17beta-hydroxysteroid dehydrogenase. *J. Biol. Chem.*, **273**, 8145–8152.
17. Sawicki, M.W., Erman, M., Puranen, T., Vihko, P. and Ghosh, D. (1999) Structure of the ternary complex of human 17beta-hydroxysteroid dehydrogenase type 1 with 3-hydroxyestra-1,3,5,7-tetraen-17-one (equilin) and NADP+. *Proc. Natl. Acad. Sci. USA*, **96**, 840–845.

18. Kowalik, D., Haller, F., Adamski, J. and Moeller, G. (2009) In search for function of two human orphan SDR enzymes: hydroxysteroid dehydrogenase like 2 (HSDL2) and short-chain dehydrogenase/reductase-orphan (SDR-O). *J. Steroid Biochem. Mol. Biol.*, **117**, 117–124.
19. Li, H. and Durbin, R. (2009) Fast and accurate short read alignment with Burrows-Wheeler transform. *Bioinformatics*, **25**, 1754–1760.
20. Li, H., Handsaker, B., Wysoker, A., Fennell, T., Ruan, J., Homer, N., Marth, G., Abecasis, G. and Durbin, R., 1000 Genome Project Data Processing Subgroup. (2009) The Sequence Alignment/Map format and SAMtools. *Bioinformatics*, **25**, 2078–2079.
21. McKenna, A., Hanna, M., Banks, E., Sivachenko, A., Cibulskis, K., Kernytsky, A., Garimella, K., Altshuler, D., Gabriel, S., Daly, M., *et al.* (2010) The Genome Analysis Toolkit: a MapReduce framework for analyzing next-generation DNA sequencing data. *Genome Res.*, **20**, 1297–1303.
22. Cingolani, P., Platts, A., Wang le, L., Coon, M., Nguyen, T., Wang, L., Land, S.J., Lu, X. and Ruden, D.M. (2012) A program for annotating and predicting the effects of single nucleotide polymorphisms, SnpEff: SNPs in the genome of Drosophila melanogaster strain w1118; iso-2; iso-3. *Fly (Austin)*, **6**, 80–92.
23. Wang, K., Li, M. and Hakonarson, H. (2010) ANNOVAR: functional annotation of genetic variants from high-throughput sequencing data. *Nucleic Acids Res.*, **38**, e164.
24. Niwa, H., Yamamura, K. and Miyazaki, J. (1991) Efficient selection for high-expression transfectants with a novel eukaryotic vector. *Gene*, **108**, 193–199.
25. Shimomura, Y., Agalliu, D., Vonica, A., Luria, V., Wajid, M., Baumer, A., Belli, S., Petukhova, L., Schinzel, A., Brivanlou, A.H., *et al.* (2010) APCDD1 is a novel Wnt inhibitor mutated in hereditary hypotrichosis simplex. *Nature*, **464**, 1043–1047.
26. Fujimoto, A., Farooq, M., Fujikawa, H., Inoue, A., Ohyama, M., Ehama, R., Nakanishi, J., Hagihara, M., Iwabuchi, T., Aoki, J., *et al.* (2012) A missense mutation within the helix initiation motif of the keratin K71 gene underlies autosomal dominant woolly hair/hypotrichosis. *J. Invest. Dermatol.*, **132**, 2342–2349.